RSC Advances

PAPER

View Article Online
View Journal | View Issue

Cite this: *RSC Adv.*, 2020, **10**, 35007

The construction of a simple sensor for the simultaneous detection of nitrite and thiosulfate by heme catalysis

Guo-Cheng Han, *[a] Huifang Li,[a] Annaleizle Ferranco,[b] Tao Zhan,[a] Yunyun Cheng,[a] Zhencheng Chen, [a] Mingyue Xue,[a] Xiao-Zhen Feng*[a] and Heinz-Bernhard Kraatz *[b]

Several simple sensors were fabricated through a one-step method. By depositing electro-active compounds, such as β-cyclodextrins (β-CD), heme, dopamine (DA), or Fc-ECG, onto a screen-printed electrode (SPE), the successful simultaneous detection of nitrite (NO_2^-) and thiosulfate ($S_2O_3^{2-}$) ions was observed. Under optimal operating conditions, the notable electrocatalytic abilities of a Heme/SPE sensor were detected for the oxidation of NO_2^- and $S_2O_3^{2-}$, with remarkable peak potential differences, after characterization *via* SEM, CV, and DPV. Linear relationships were obtained in the ranges of 5.0–200.0 μmol L^{-1} and 1.0–100.0 μmol L^{-1} for the current response *versus* concentration of NO_2^- and $S_2O_3^{2-}$, respectively. The limits of detection were determined to be 1.67 and 0.33 μmol L^{-1} while the sensitivities of detection were noted to be 0.43 and 1.43 μA μM^{-1} cm^{-2}, respectively. During the detection of NO_2^- and $S_2O_3^{2-}$, no interfering common ions were observed. Furthermore, average recoveries from 96.0 to 104.3% and a total R.S.D. of less than 3.1% were found for the detection of NO_2^- and $S_2O_3^{2-}$ in pickled juice and tap water using the simple sensor. These results showed that rapid and precise measurements for actual application in NO_2^- and $S_2O_3^{2-}$ detection could be conducted in food samples, indicating a potential use in food safety.

Received 12th August 2020
Accepted 10th September 2020

DOI: 10.1039/d0ra06942f

rsc.li/rsc-advances

1. Introduction

It is well known that nitrite (NO_2^-) can cause cancer under the action of gastric acid; NO_2^- can react with nontoxic secondary amines and amides in food to form carcinogenic nitrosamines. NO_2^- is often added to fresh meat and fish products for food preservation since it is a good antimicrobial agent, which aids in the prevention of natural degradation.[1] Excessive intake of NO_2^- can lead to death since NO_2^- can react with the trivalent iron of hemoglobin, reducing it to sub hemoglobin, leading to tissue hypoxia, and thus causing death.[2,3] Therefore, NO_2^- is a highly toxic ion.[4] NO_2^- is also listed as an important pollutant in many countries. Because its appearance is similar to that of salt, some lawbreakers will use NO_2^- to make fake salt.[5,6]

Sodium thiosulfate ($Na_2S_2O_3$) can be produced by thiosulfate ($S_2O_3^{2-}$) and sodium metal. $S_2O_3^{2-}$ can also be used for applications in medical treatment, such as the detoxification of cyanide. Thiocyanase, which is found in the body, can combine $S_2O_3^{2-}$ with the toxic cyanide ion to form the nontoxic thiocyanate which can subsequently be discharged through urine, preventing cyanide from harming the human body.[7] There are other uses for $S_2O_3^{2-}$ other than metal detoxification and gold and/or silver leaching, including the treatment of some skin diseases. It is also widely used in biochemistry, environmental treatment, and other fields.[8,9]

NO_2^- and $S_2O_3^{2-}$ can affect the human body: excessive intake of NO_2^- can lead to death, but $S_2O_3^{2-}$ can also be used in the detoxification of cyanide. So how to detect the mixture of NO_2^- and $S_2O_3^{2-}$ accurately and sensitively has a certain significance for food safety and human health.[10,11]

Numerous analytical techniques are used for the detection of NO_2^- and $S_2O_3^{2-}$ with good sensitivity. Some of the common hyphenated techniques include gas chromatography-mass spectrometry (GC-MS),[12,13] liquid chromatography-mass spectrometry (LC-MS),[14,15] HPLC,[16] fluorescence detection,[17] and electrochemical methods.[18]

Electrochemical techniques are ideal analytical and detection methods because of their sensitive response, rapid detection, simple operation, low cost, and portability.[19,20] The main mode of detection is based on the oxidation of both NO_2^- and $S_2O_3^{2-}$ on the surface of the electrode or the reaction with a probe that is capable of enhancing the electrochemical signal. For electrochemical detection, something to consider when creating a modified electrode is that it should be able to possess

[a]*School of Life and Environmental Sciences, Guilin University of Electronic Technology, Guilin 541004, P. R. China. E-mail: hangc81@guet.edu.cn; fxz97118@guet.edu.cn*
[b]*Department of Physical and Environmental Sciences, University of Toronto Scarborough Campus, Toronto, Ontario M1C 1A4, Canada. E-mail: bernie.kraatz@utoronto.ca*

a charge transport capability in order to acquire a strong response. Obtaining a suitable catalyst-modified electrode should lead to enhanced catalytic activity for NO_2^- and $S_2O_3^{2-}$ detection. Shabani-Nooshabadi *et al.* reported a sensor for 4-chlorophenol that used a graphene oxide NiO/NPs-ionic liquid (*n*-hexyl-3-methylimidazolium hexafluoro phosphate) carbon paste electrode. The proposed sensor was used for the determination of 4-chlorophenol in the presence of nitrite. It exhibited a strong enhancement effect on 4-chlorophenol and showed superior catalytic activity towards the electro-oxidation of 4-chlorophenol.[21] Shabani-Nooshabadi *et al.* were able to analyze thiosulfate, 4-chlorophenol and nitrite in mixed samples using a voltammetric sensor. Through a combination of the highly conductive properties of NiO nanoparticles and a novel catechol derivative (2,4-dimethyl-*N*′-[1-(2,3-dihydroxyphenyl)methylidene]aniline) (2,4-DDMA) that has excellent mediator properties, the simultaneous analysis of thiosulfate, 4-chlorophenol and nitrite was achieved with a limit of detection of 0.01 μM for thiosulfate, of 0.7 μM for 4-chlorophenol, and of 5.0 μM for nitrite.[18] Jahan Bakhsh Raoof *et al.* fabricated a 2,7-bis(ferrocenylethyl)-fluoren-9-one-modified carbon paste electrode (2,7-BFEFMCPE) for the electrocatalytic oxidation of thiosulfate in which a detection limit of 0.15 μM was obtained.[22] All the reported compounds were used as catalysis materials, which possess an electrocatalytic property, but they were very complex compounds that cannot be obtained easily.

In this article, we report a facile process for the construction of a modified screen-printed electrode (SPE) by the direct deposition of easily obtained electro-active materials, including β-cyclodextrins (β-CD), heme, dopamine (DA), or Fc-ECG, onto SPE for the simultaneous detection of NO_2^- and $S_2O_3^{2-}$. Easily fabricated sensors, β-CD/SPE, Heme/SPE, DA/SPE and Fc-ECG/SPE, were acquired. Nonetheless, the results indicated that the Heme/SPE sensor displayed the highest oxidation peak current with remarkable peak potential differences for the simultaneous detection of NO_2^- and $S_2O_3^{2-}$ when compared to the other sensors. The presence of heme on SPE can improve the electrocatalytic activity of the bare electrode. Investigations with Heme/SPE were conducted to determine the most effective concentrations of NO_2^- and $S_2O_3^{2-}$. Further investigations using the proposed method were also undertaken to detect NO_2^- and $S_2O_3^{2-}$ in pickled juice and tap water, which led to satisfactory results.

2. Experimental

2.1 Reagents

β-Cyclodextrins (β-CD), heme, dopamine (DA), ascorbic acid (AA), sodium thiosulfate ($Na_2S_2O_3$) and sodium nitrite ($NaNO_2$) were purchased from Aladdin Reagent Co. Ltd. (Shanghai, China). Synthetic Fc[CO-Glu-Cys-Gly-OH] (Fc-ECG), electro-active material, was prepared by Jier Biochemistry Co. Ltd. in Shanghai, China. A local supermarket provided pickled mustard. All the screen-printed electrodes (SPEs) were obtained from Nanjing Yunyou Biotechnology Co. Ltd. Milli-Q water was used to prepare all aqueous solutions. All other chemicals, unless stated otherwise, were used directly without further purification and were analytical grade reagents.

2.2 Instrumentation

Characterization for surface morphologies of each sensor was conducted using a field emission scanning electron microscope (Japan High Technology Company) and the measurements were obtained at a working distance of 6000 μm at 3 kV and 10 100 nA.

A three-electrode system was used to conduct electrochemical analyses, where the counter, reference and working electrodes were a carbon electrode, an Ag wire, and the modified carbon electrode (φ = 3 mm), respectively. The obtained data were acquired using a CHI660E electrochemical workstation (Shanghai Chenhua Instrument Co., Ltd., China), which was attached to the three-electrode system for testing. The CV experiments were conducted in 0.1 mol L^{-1} PBS as the supporting electrolyte with a 100 mV s^{-1} scan rate and the parameters were set to scan from 0 to 1200 mV. The DPV experiments were conducted and the parameters were set to scan in the range from 0 to 1000 mV and 50 mV as the pulse amplitude. In addition, EIS measurements were conducted using a frequency range of 100 000 to 0.1 Hz, an amplitude of 5 mV, an initial voltage of 300 mV, and with open circuit potentials. An initial voltage of 100 mV was recorded for the electrochemical *i*–*t* curve.

2.3 Electrochemical measurements for NO_2^- and $S_2O_3^{2-}$ by modification of the electrode

100 mmol L^{-1} stock solutions of NO_2^- and $S_2O_3^{2-}$ were prepared by dissolving sodium nitrite and sodium thiosulfate using Milli-Q water. A concentration of 10.0 mmol L^{-1} of heme stock solution was made by dissolving heme in a basic solution (pH 8.0). In order to prepare the other individual stock solutions, β-CD, DA or Fc-ECG were dissolved in Milli-Q water at a concentration of 0.5 mmol L^{-1}. 0.1 mol L^{-1} PBS solution was used as the supporting electrolyte and the pH of the solution was adjusted by adding either 0.1 mol L^{-1} of H_3PO_4 or NaOH solution. The prepared solutions were stored at 4 °C and the required dilutions were prepared prior to use. The *i*–*t* technology was used to deposit the electro-active materials, heme, DA, β-CD or Fc-ECG, directly onto the SPE surface with an initial voltage of 100 mV for 200 s to prepare all the sensors. The facile preparation of the Heme/SPE electrochemical sensor by the DPV technique is depicted in Scheme 1 and the sensor was used for the simultaneous detection of NO_2^- and $S_2O_3^{2-}$.

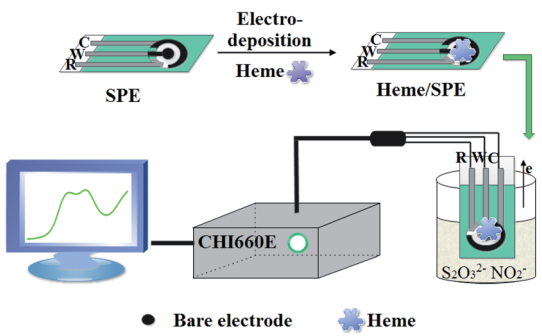

Scheme 1 The fabrication of the Heme/SPE sensor by the DPV technique for the detection of NO_2^- and $S_2O_3^{2-}$.

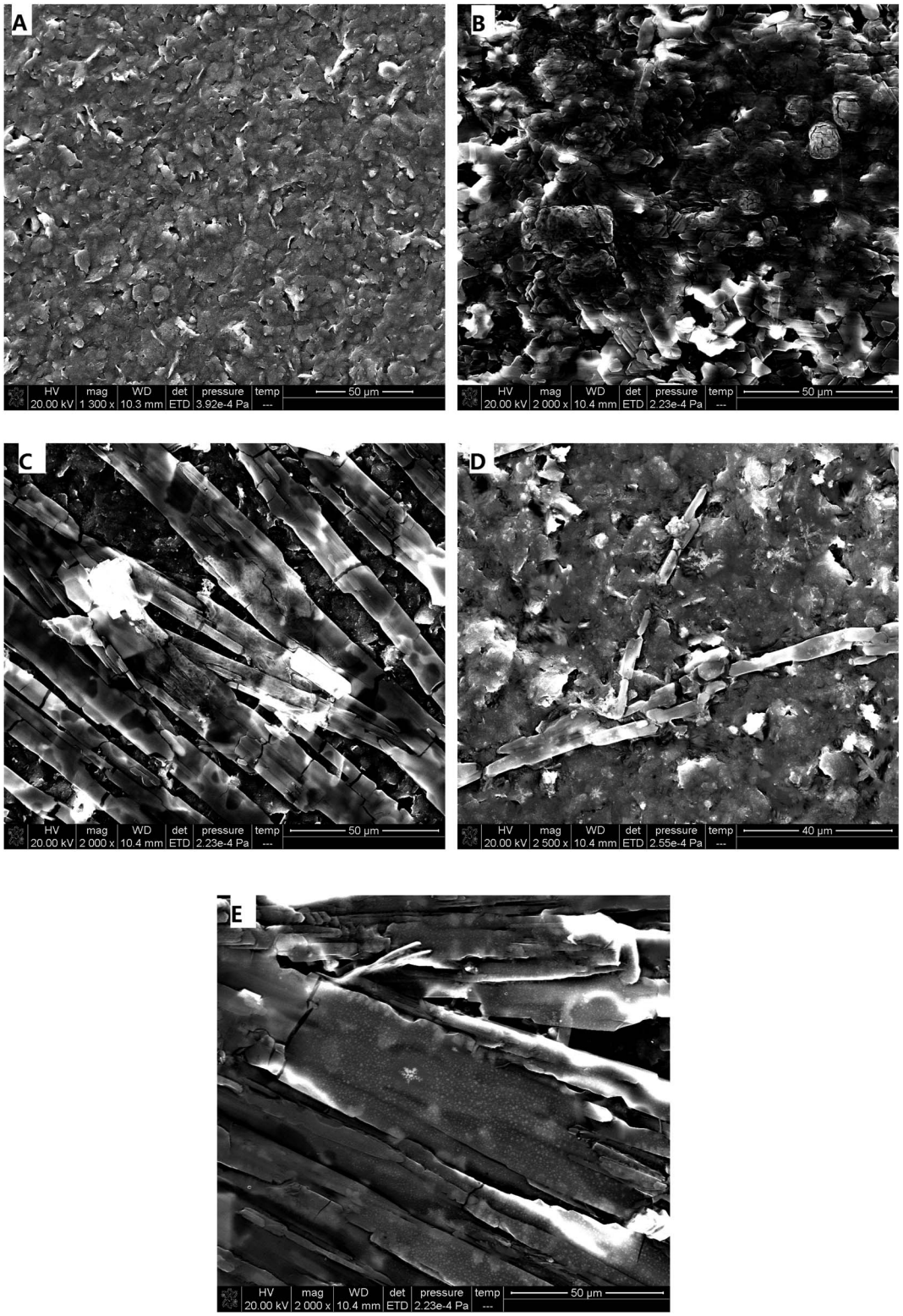

Fig. 1 SEM images of different modified electrodes ((A): naked SPE; (B): β-CD/SPE; (C): DA/SPE; (D): Fc-ECG/SPE; (E): Heme/SPE).

3. Results and discussion

3.1 Characterization and properties of the modified electrodes

In order to obtain a remarkable electrochemical response, electrochemical media were used to make the modified electrodes and enhance the electrocatalytic effects. Herein, the electrochemical media β-CD, heme, DA, and Fc-ECG were chosen to fabricate four different sensors. Upon deposition of electro-active materials, SEM was carried out to elucidate the electrode surface. Fig. 1 depicts the different modified electrodes through SEM images.

A significant number of rough amorphous carbon particles were observed on the surface morphology of naked SPE, as shown in Fig. 1A, and all the pure carbon particles look very smooth, like a platform. After separately depositing four different types of electro-active materials, β-CD, DA, Fc-ECG, and heme, onto SPE, each modified electrode appeared to be dissimilar. As demonstrated in Fig. 1B, multiple flower buds could be observed on the electrode surface without uniformity, and it looked very different from the carbon particles. In contrast, bamboo clusters, sparse dendritic rods, and strip stones coated the surfaces of the electrodes shown in Fig. 1C, D and E when the electro-active materials DA, Fc-ECG and heme were deposited, respectively. Through one-step deposition, the modified electrode surfaces differ from each other. In addition, successful coating of the electro-active materials was observed for each SPE surface.

After surface morphology characterization of the as-prepared sensors, the report subsequently directed its focus towards the electro-active response property for potential applications. The DPV results shown in Fig. 2 were measured in 0.1 mol L^{-1} PBS (pH 7.0) and DPV curves are displayed for SPE, β-CD/SPE, DA/SPE, Fc-ECG/SPE and Heme/SPE (A). Additionally, Fig. 2 also shows EIS curves of the naked and modified electrodes in 5.0 mmol L^{-1} potassium ferricyanide solution present in 0.1 mol L^{-1} KCl as the electrolyte (B).

In Fig. 2A, curves (a) and (b) display an almost straight line without an electrocatalytic response. It is apparent in Fig. 2A that the other curves were all observed to possess electrocatalytic responses from DA/SPE, Fc-ECG/SPE and Heme/SPE in PBS. PBS was used as the blank when DA, Fc-ECG and heme modified electrodes were examined and exhibited positive oxidation peaks at 0.15, 0.30 and 0.70 V, with 0.98, 1.72 and 3.25 μA weak peak current responses, respectively, which corresponded to their internal electrocatalytic performance. Fig. 2B displays common EIS curves for each individual sensor examined in a solution of potassium ferricyanide. Sensors DA/SPE and Fc-ECG/SPE showed relatively large impedances (Fig. 2B(c and d)), indicating that the electron transfer was hampered in the electrochemical process for each modified electrode, suggesting that the medium in which DA and Fc-ECG were present shows low electro-activity in ferricyanide solution. On the other hand, after depositing electro-active materials β-CD and heme on the naked electrode, the impedances remain almost the same, indicating that electron transfer was not significantly hindered compared to sensors DA/SPE and Fc-ECG/SPE. By comparing the electron transfer ability of the modified electrodes, it was observed that both β-CD/SPE and Heme/SPE sensors showed ideal electronic transmitting abilities.

3.2 Electrochemical studies

Detection of NO_2^- and $S_2O_3^{2-}$ for actual application was investigated upon characterization of the electrochemical sensors. Fig. 3 shows CV curves (A, B and C) and DPV curves (D, E and F) of 100 μmol L^{-1} NO_2^- (A and D), 50 μmol L^{-1} $S_2O_3^{2-}$ (B and E), and NO_2^- and $S_2O_3^{2-}$ mixed solutions (C and F), which were catalyzed by various modified electrodes using PBS at pH 7.0.

In Fig. 3A and B, an electrochemical signal for the oxidation of two separate solutions containing NO_2^- and $S_2O_3^{2-}$ was observed on the surfaces of five sensors in the range of 0.6–0.8 and 0.8–1.0 V, respectively, but not one sensor showed remarkable current responses toward the two analytes. In Fig. 3C, similar values for NO_2^- and $S_2O_3^{2-}$ were observed since only one oxidation peak appeared when investigating the detection of NO_2^- and $S_2O_3^{2-}$ mixed solutions using each of the five sensors: naked SPE, β-CD/SPE, DA/SPE, Fc-ECG/SPE, and Heme/SPE. Therefore, none of the modified sensors was used to measure the detection of NO_2^- and $S_2O_3^{2-}$ by the CV technique with lower sensitivity since two distinguishable signals were not observed. Consequently, DPV was employed

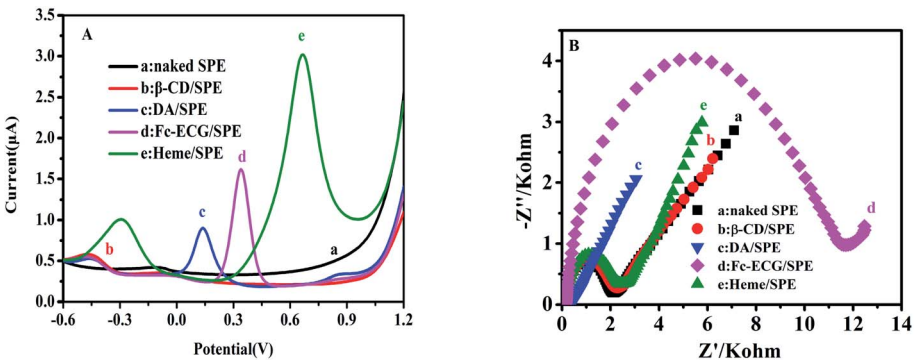

Fig. 2 DPV curves from SPEs modified with different materials in PBS (pH 7.0) (A) and EIS curves from SPEs modified with different materials in $K_4Fe(CN)_6/K_3Fe(CN)_6$ solution (B) ((a): naked SPE; (b): β-CD/SPE; (c): DA/SPE; (d): Fc-ECG/SPE; (e): Heme/SPE).

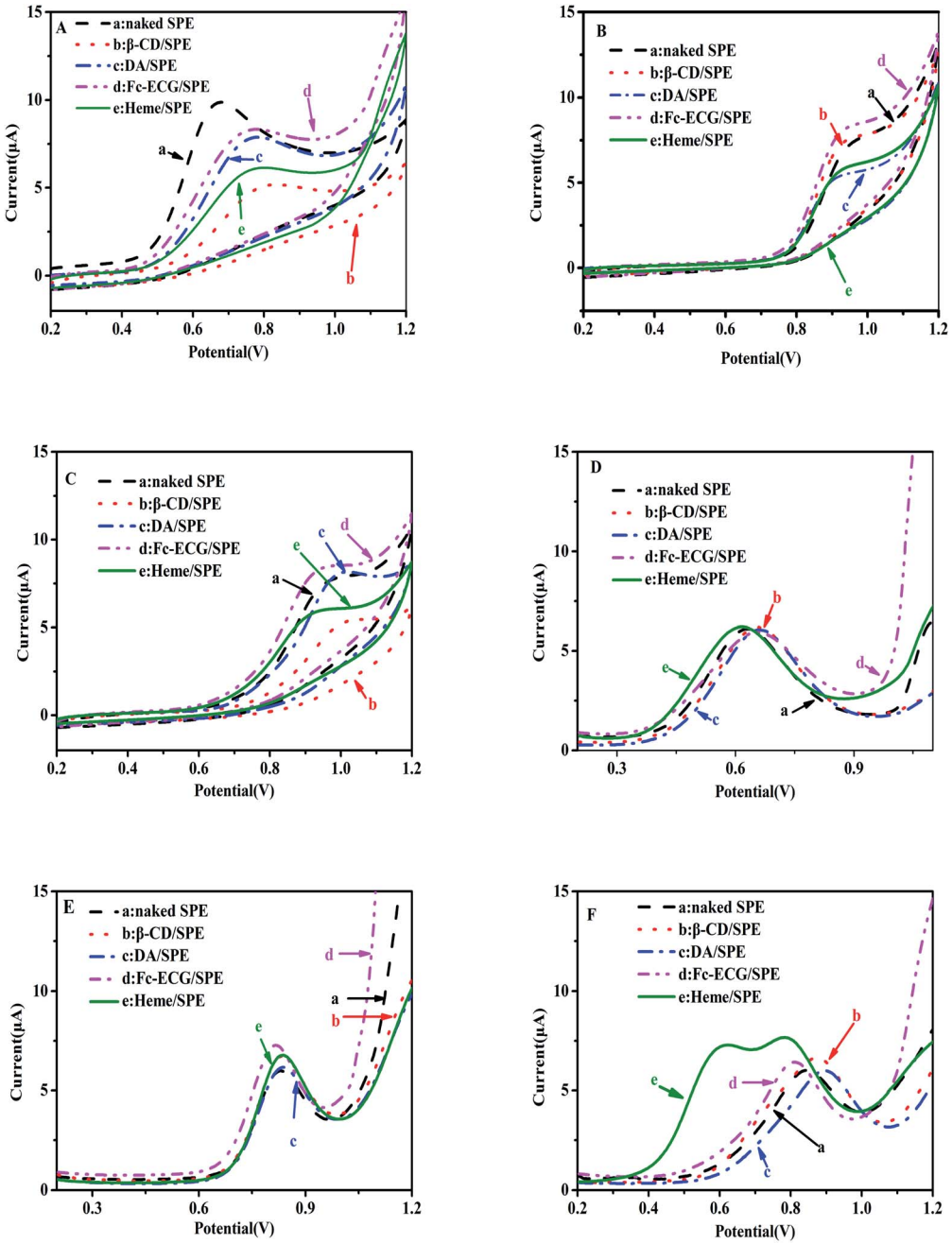

Fig. 3 CV graphs (A–C) and DPV curves (D–F) of various naked and modified sensors for the detection of 100 μmol L^{-1} NO_2^- (A and D), 50 μmol L^{-1} $S_2O_3^{2-}$ (B and E), and mixed solutions (C and F) in 0.1 mol L^{-1} PBS (pH 7.0) ((a): naked SPE; (b): β-CD/SPE; (c): DA/SPE; (d): Fc-ECG/SPE; (e): Heme/SPE).

to detect NO_2^- and $S_2O_3^{2-}$ in a solution mixture. Fig. 3D and E indicate that no remarkable current response appears for two separate solutions containing either NO_2^- or $S_2O_3^{2-}$. In a mixed solution containing NO_2^- and $S_2O_3^{2-}$, the following sensors, naked SPE, β-CD/SPE, DA/SPE, Fc-ECG/SPE, still showed one oxidation of two ions to confirm no catalysis effect from the medium towards oxidation of NO_2^- and $S_2O_3^{2-}$. However, it was exciting that two separated peaks were observed on the Heme/SPE sensor (curve (e) in Fig. 3F). The DPV results showed separate electrochemical signals for the oxidation of each of NO_2^- and $S_2O_3^{2-}$ in a solution mixture. An enhancement in the current response was also observed for the Heme/SPE sensor compared to the other sensors. Therefore, the Heme/SPE sensor was revealed to be the most suitable sensor for NO_2^- and $S_2O_3^{2-}$ catalysis due to heme with its compact rod shapes possessing a larger surface area and more active sites which can promote the charge transfer on the electrode. Our group previously reported that the Heme/SPE sensor enhanced current responses for UA, AA, DA and BPA catalysis due to the electrocatalytic ability of heme.[23,24] As

a result, Heme/SPE exhibits advantageous catalytic capabilities for oxidation of NO_2^- and $S_2O_3^{2-}$. Additional analyses examining the ability for detection of NO_2^- and $S_2O_3^{2-}$ were consequently undertaken.

3.3 Optimization studies

Several experimental conditions were investigated with the intention of determining the optimal experimental settings. The following conditions were investigated: the ideal concentration of heme for deposition, deposition time, optimal pH, and detection temperature. Fig. 4A and B show the current responses as the concentration of heme changed and with differing deposition times of heme, respectively. Fig. 4C displays the current response for different pH values of PBS. Fig. 4D shows the current responses for different temperatures. The inserts depicted in Fig. 4A–D show the DPV curves of the Heme/SPE sensor for oxidation of NO_2^- and $S_2O_3^{2-}$ as the concentration of heme changed, for differing deposition times of heme, different pH values of PBS, and different temperatures, respectively.

The effects of deposition concentrations from 0.25 to 2.0 mM of the electro-active material heme for catalysis of NO_2^- and $S_2O_3^{2-}$ are demonstrated in Fig. 4A. The observed results showed notable values that 1.0 mmol L^{-1} of heme led to the highest current response while the responses for the other concentrations that were investigated showed lower responses. As a result, 1.0 mmol L^{-1} concentration was selected for subsequent investigations. Based on these results, lower concentrations of heme showed that the electrode was incapable of suitably catalyzing NO_2^- and $S_2O_3^{2-}$. However, increased concentrations greater than 1.0 mmol L^{-1} heme led to ineffective electron transfer as the electrode became hampered. As shown in Fig. 4B, increased the deposition time of heme onto the electrode surface led to the current value increasing. The largest current response was observed at 200 s, indicating that this time was the value at which the most effective enrichment of heme would take place on the electrode surface. For that reason, the preferred preparation time for heme deposition was 200 s. An additional condition to investigate when establishing the ideal conditions for detection of NO_2^- and $S_2O_3^{2-}$ is determining the ideal pH value. As demonstrated in Fig. 4C, at pH = 7.0, the Heme/SPE sensor exhibited the highest current responses for oxidation peaks of NO_2^- and $S_2O_3^{2-}$. At higher pH values, the shortage of protons caused decreased oxidation peak currents and the electrocatalytic oxidation of NO_2^- and $S_2O_3^{2-}$ became affected. However, a noticeably decreased peak current was observed under lower pH conditions, indicating that more acidic environments caused the formation of nitrous acid and thiosulfuric acid, reducing the amount of NO_2^- and $S_2O_3^{2-}$ available for oxidation. Lastly, two distinct oxidation peaks and maximum oxidation peak currents were observed at pH 7. Consequently,

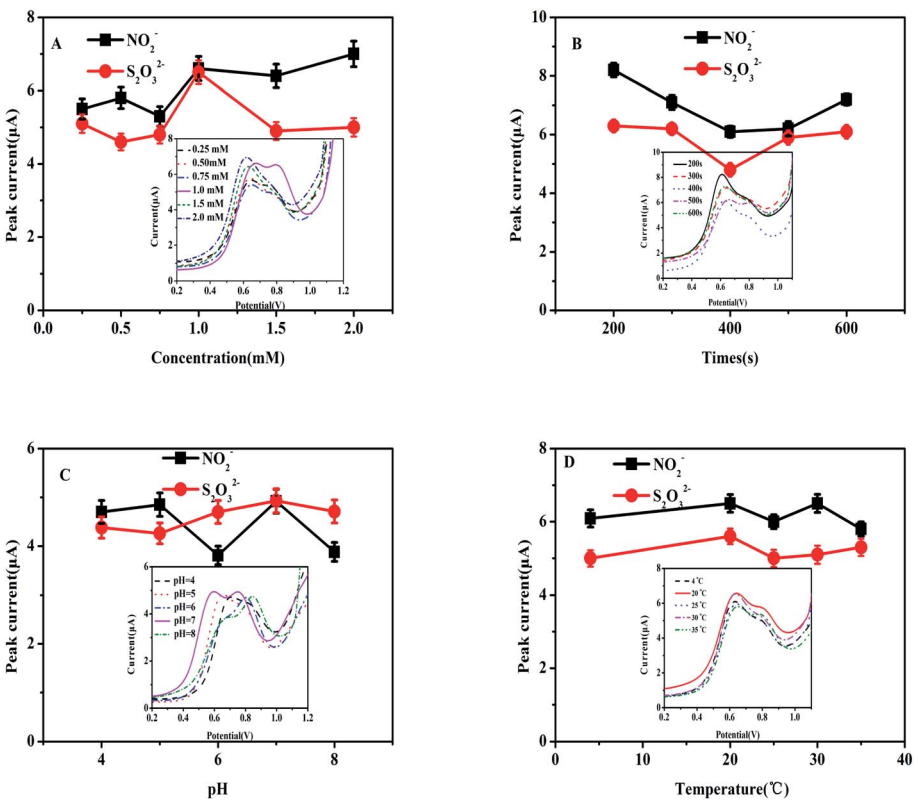

Fig. 4 Plots of the Heme/SPE sensor current responses for the oxidation of NO_2^- and $S_2O_3^{2-}$ (50 μmol L^{-1}) in PBS (0.1 mol L^{-1}) (the inserts are the DPV curves). ((A): pH 7.0, with the deposition of different concentrations of heme at 25 °C; (B): pH 7.0, with different heme deposition times at 25 °C; (C): pH 4.0, 5.0, 6.0, 7.0, and 8.0, at 25 °C; (D): pH 7.0, at 4, 20, 25, 30, and 35 °C).

further electrochemical analyses were carried out at pH 7 as the ideal condition. As depicted in Fig. 4D, the temperature did not appear to remarkably affect the current response. Therefore, subsequent studies were investigated at 25 °C (room temperature) for oxidation of NO_2^- and $S_2O_3^{2-}$.

3.4 NO_2^- and $S_2O_3^{2-}$ detection assays

As discussed previously, the key goal of this report was to develop and construct a facile electrochemical sensor in order to simultaneously detect both NO_2^- and $S_2O_3^{2-}$ in solution as the DPV technique was applied. Fig. 5A shows the DPV curve for varying concentrations of NO_2^- and $S_2O_3^{2-}$ in a solution mixture using the Heme/SPE sensor in PBS. Fig. 5B and C display the relationship between current response and separate NO_2^- and $S_2O_3^{2-}$ solution concentrations, respectively, with a wide range detected by the Heme/SPE sensor.

Fig. 5A shows the amperometric responses against different concentrations of NO_2^- and $S_2O_3^{2-}$ mixed solutions with the Heme/SPE sensor and includes calibration plots of current response and concentrations. It can be observed that the Heme/SPE sensor gave two distinct oxidation peaks at 0.60 V and 0.80 V under optimal conditions with peak potential differences of 200 mV from NO_2^- and $S_2O_3^{2-}$. In addition, the current responses of the sensor increased with linearly when the NO_2^- and $S_2O_3^{2-}$ concentration increased. Hence, the Heme/SPE sensor was entirely capable of the simultaneous detection of NO_2^- and $S_2O_3^{2-}$. Electrochemical oxidation peaks for NO_2^- and $S_2O_3^{2-}$ were further enhanced as the concentration increased over a broad range and an established linear relationship was observed, as shown in Fig. 5B and C. A strong linear relationship was obtained between the NO_2^- concentration and the current: the linear equation was $I = 4.05227 + 0.02909c$ (I is the current, and c is concentration) with the correlation coefficient determined to be 0.99714; the linear range was between 5.0 and 200.0 μmol L^{-1}; the limit of detection was 1.67 nmol L^{-1}, and the sensitivity of detection was 0.43 μA μM^{-1} cm^{-2}. For analysis of $S_2O_3^{2-}$ using the same method, the linear equation was $I = 1.31585 + 0.10262c$, with correlation coefficient 0.99783, the linear range was between 1.0 and 100.0 μmol L^{-1} with 0.33 nmol L^{-1} limit of detection and 1.43 μA μM^{-1} cm^{-2} sensitivity of detection. Table 1 displays a comparison for the detection of NO_2^- and $S_2O_3^{2-}$ by

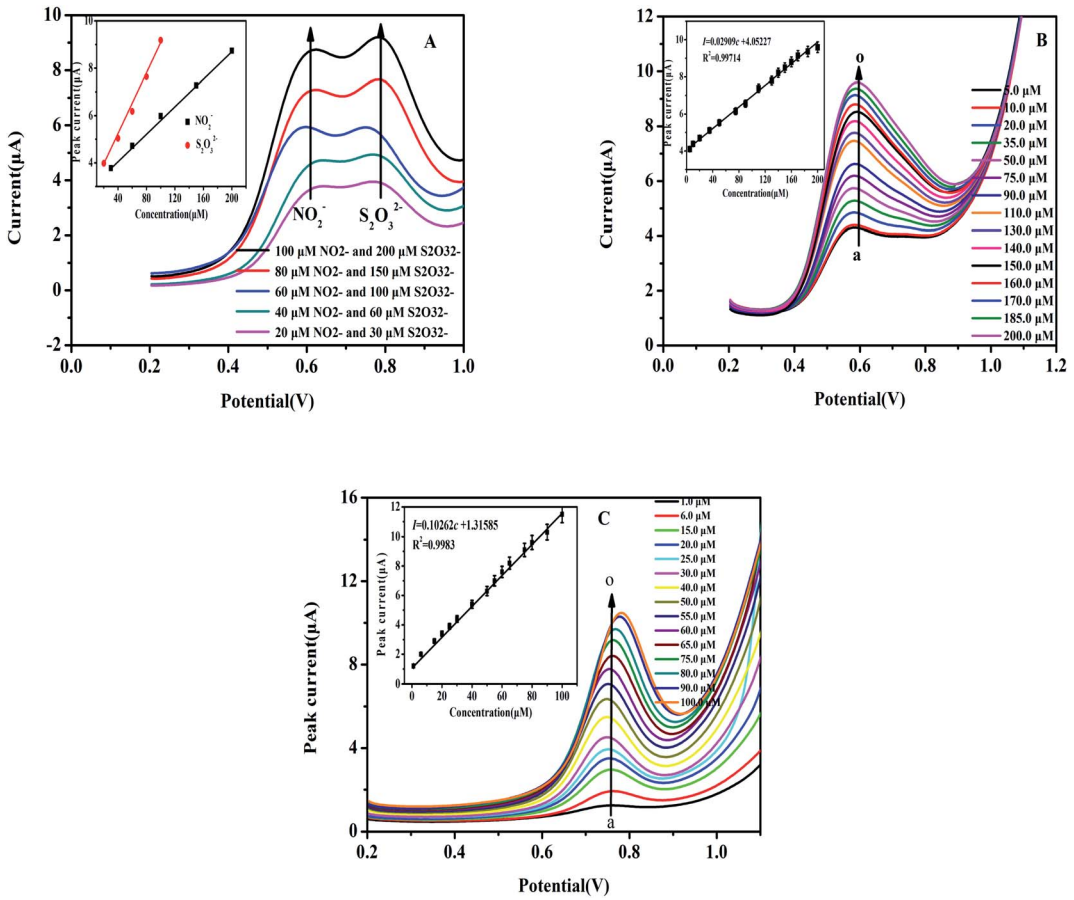

Fig. 5 (A): DPV diagrams of varying concentrations of NO_2^- and $S_2O_3^{2-}$ mixed solutions on Heme/SPE (NO_2^-: 20.0, 40.0, 60.0, 80.0, and 100.0 μmol L^{-1}; $S_2O_3^{2-}$ 30.0, 60.0, 100.0, 150.0, and 200.0 μmol L^{-1}); (B): DPV diagrams of different NO_2^- concentrations on Heme/SPE ((a–o): 5.0, 10.0, 20.0, 35.0, 50.0, 75.0, 90.0, 110.0, 130.0, 140.0, 150.0, 160.0, 170.0, 185.0, and 200.0 μmol L^{-1}); (C): DPV diagrams of different $S_2O_3^{2-}$ concentrations on Heme/SPE ((a–o): 1.0, 6.0, 15.0, 20.0, 25.0, 30.0, 40.0, 50.0, 55.0, 60.0, 65.0, 75.0, 80.0, 90.0, and 100.0 μmol L^{-1}); insets: calibration plots showing current *vs.* concentration.

Table 1 A comparison of the detection of NO_2^- and $S_2O_3^{2-}$ with modified electrodes

Modified electrode	Analytical method	Detection limit (μM)		Linear range (μM)		Ref.
		NO_2^-	$S_2O_3^{2-}$	NO_2^-	$S_2O_3^{2-}$	
2,4-DDMA-NiO/NP/CPE	SWV	5.0	0.01	10.0–700.0	0.05–400.0	18
2,7-BFEFMCPE	DPV		0.15		0.6–90.0	22
CdO/NPs/CNDPMA/CPE	SWV		0.04		0.09–350	25
CdO/SWCNTs/MBIB/CPE	SWV	0.07		0.1–900.0		26
CoPc/MWCNTs	DPV	2.11		10.0–1.05 × 10^6		27
Heme/SPE	DPV	1.67	0.33	5.0–200.0	1.0–100.0	This work

other modified electrodes. The method investigated in this report was made simpler based on the construction of the one-step fabricated electrochemical sensor: by depositing heme, an easily obtained compound, onto the SPE for detection of NO_2^- and $S_2O_3^{2-}$.

3.5 Selectivity, repeatability, and stability studies

An electrochemical sensor must possess strong selectivity and stability for application purposes, as well as repeatability.[28–32] The possibility of interfering ions was investigated to determine the selectivity of the Heme/SPE sensor towards NO_2^- and $S_2O_3^{2-}$. Different types of compounds were examined, including glucose, AA, Na_2SO_4, $NaNO_3$, and KCl (100 μmol L^{-1}) in food samples to study the selectivity of the sensor. Fig. 6A and B present *i–t* curves of amperometric responses of NO_2^- and $S_2O_3^{2-}$ with glucose, AA, Na_2SO_4, $NaNO_3$, and KCl, respectively. First of all, upon addition of a three-fold amount of both NO_2^- and $S_2O_3^{2-}$ three-fold currents were observed. Secondly, when different interfering compounds were added, no changes in current were detected, indicating that the as-prepared sensor possessed reliable selectivity for detection of NO_2^- and $S_2O_3^{2-}$. Lastly, another characteristic included in this study was the stability of the Heme/SPE sensor. Upon modification of the Heme/SPE, its application for detection of the same concentrations of NO_2^- and $S_2O_3^{2-}$ with various times was studied. As depicted in Fig. 6C, the as-prepared sensor revealed peak currents at 0.60 and 0.80 V toward oxidation of NO_2^- and $S_2O_3^{2-}$. The Heme/SPE was stored and after 6 days of storage, no observable changes were observed for peak current intensities, and the values of R.S.D. for current intensity were 3.98% and

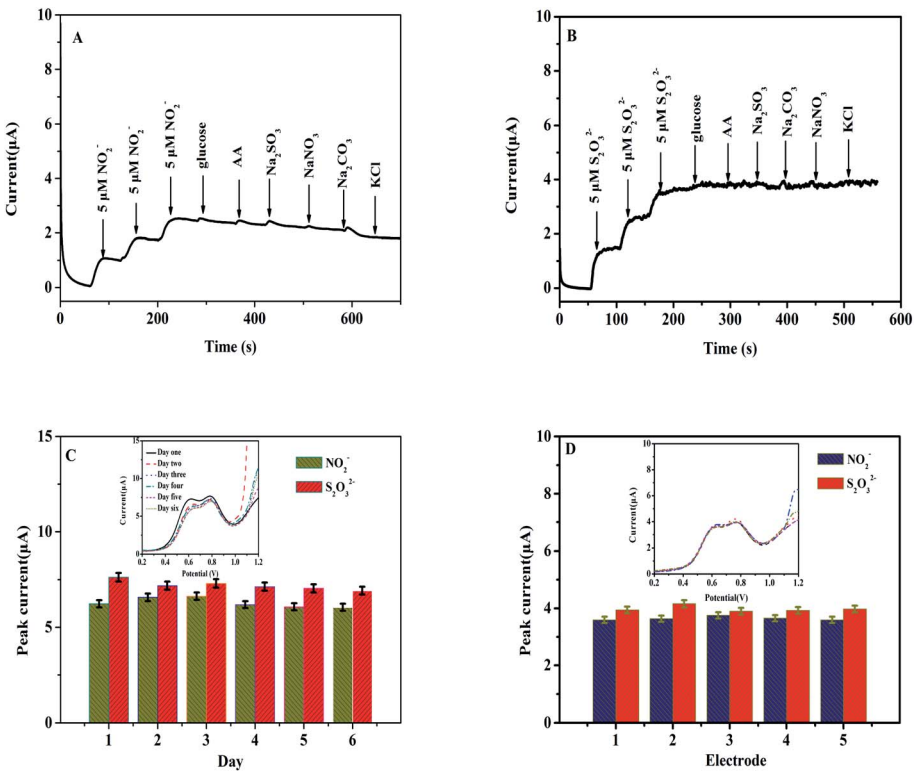

Fig. 6 (A): The selectivity diagram of the Heme/SPE sensor for NO_2^-; (B): the selectivity diagram of the Heme/SPE sensor for $S_2O_3^{2-}$; (C): the stability diagram of the Heme/SPE sensor; and (D): the repeatability diagram of the Heme/SPE sensor.

Table 2 Results of NO_2^- and $S_2O_3^{2-}$ detection in real samples ($n = 5$)[a]

Analyte		Detected (μmol L^{-1})	Added (μmol L^{-1})	Average Found (μmol L^{-1})	Average Recovery (%)	RSD (%)		
						Average	Intra-assay	Inter-assay
Pickled juice	NO_2	16.8 ± 0.3	20.0, 40.0, 60.0	35.7 ± 0.4, 57.2 ± 0.5, 77.8 ± 0.4	98.0, 100.7, 101.3	1.6, 3.2, 2.8	2.5	3.1
	$S_2O_3^{2-}$	—	20.0, 40.0, 60.0	19.2 ± 0.5, 38.7 ± 0.8, 58.9 ± 0.3	96.0, 96.7, 98.2	2.5, 2.9, 4.3	3.2	
Tap water	NO_2^-	—	20.0, 40.0, 60.0	19.5 ± 0.5, 39.9 ± 0.8, 61.9 ± 0.3	97.5, 99.8, 103.2	3.2, 4.1, 2.3	3.2	
	$S_2O_3^{2-}$	—	20.0, 40.0, 60.0	19.8 ± 0.4, 41.7 ± 0.6, 62.2 ± 0.4	99.0, 104.3, 103.7	2.7, 3.8, 4.1	3.5	

[a] — not detected.

3.41%, respectively. Therefore, the development of a facile electrochemical sensor suitably detected NO_2^- and $S_2O_3^{2-}$ and possessed a high stability. Finally, five Heme/SPE sensors were independently prepared to conduct repeatability analysis. As shown in Fig. 6D, the peak currents also showed no observable change. The values were used to calculate R.S.D. of 1.79% and 2.63% for current intensity for oxidation of NO_2^- and $S_2O_3^{2-}$. This indicated that the electrochemical sensor possesses remarkable repeatability. Therefore, the design of the Heme/SPE sensor demonstrated highly favorable selectivity and feasible stability, and it was suitable for the instantaneous detection of a mixture containing NO_2^- and $S_2O_3^{2-}$ ions.

3.6 Analysis of real water samples

To verify its feasibility for practical applications, a Heme/SPE sensor was prepared to detect the presence and quantity of NO_2^- and $S_2O_3^{2-}$ concentrations in pickled juice and tap water. Additionally, the standard addition method was conducted in order to verify the application.[31,32] The samples were spiked with known amounts of NO_2^- and $S_2O_3^{2-}$ solutions (20.0, 40.0, 60.0 μmol L^{-1}). The data in Table 2 showed that the average recovery of spiked samples was from 96.0 to 104.3% while 3.1% was obtained for the inter-assay R.S.D. for response currents. This indicated that the as-prepared sensors possess the potential for practical application in real samples.

4. Conclusions

We reported a both simple and facile method for constructing a Heme/SPE sensor for the detection of NO_2^- and $S_2O_3^{2-}$ in pickled juice and tap water. Its fabrication included the direct deposition of the electro-active material heme on SPEs by an *i–t* technique. Based on the reported results, the characteristic signal of the Heme/SPE sensor showed enhanced electrocatalytic sensing towards the oxidation of NO_2^- and $S_2O_3^{2-}$ by increasing the peak current. This is attributable to heme having compact rod shapes possessing a larger surface area and more active sites and so being capable of promoting charge transfer, which acts as an electron transfer medium. The Heme/SPE sensor possesses good selectivity and appears to be an encouraging electrochemical sensor for electrocatalytic applications involving the oxidation of NO_2^- and $S_2O_3^{2-}$. In pickled juice and tap water, the inter-assay R.S.D. of detection of NO_2^- and $S_2O_3^{2-}$ was determined to be 3.1% and the average recovery ranged from 96.0 to 104.3%. This proved that the use of the Heme/SPE sensor is a valid approach for real-world applications.

Conflicts of interest

The authors declare no competing financial interests.

Acknowledgements

We gratefully acknowledge the financial support afforded by the following organizations: the National Natural Science Foundation of China (No. 61661014, 61627807, 61861010, 81873913), the Nature Science Foundation of Guangxi Province (No. 2018GXNSFAA281198, 2018GXNSFBA281135), and, finally, Guangxi One Thousand Young and Middle-aged College and University Backbone Teachers Cultivation Program. This work could not have been accomplished without their support and for that we are immensely appreciative.

References

1 M. E. E. Alahi, S. C. Mukhopadhyay and L. Burkitt, *Sens. Actuators, B*, 2018, **259**, 753–761.
2 A. D. Arulraj, E. Sundaram, V. S. Vasantha and B. Neppolian, *New J. Chem.*, 2018, **42**, 3748–3757.
3 S. Kesavan, D. R. Kumar, M. L. Baynosa and J. J. Shim, *Mater. Sci. Eng., C*, 2018, **85**, 97–106.
4 X. Z. Feng, A. Ferranco, X. R. Su, Z. C. Chen, Z. L. Jiang and G. C. Han, *Sensors*, 2019, **19**, 268.
5 B. Juskowiak, E. Galezowska and W. Szczepaniak, *Mikrochim. Acta*, 1996, **122**, 183–194.
6 S. Lu, Z. R. Gu, M. Hummel, Y. Zhou, K. L. Wang, B. B. Xu, Y. C. Wang, Y. F. Li, X. Q. Qi and X. T. Liu, *J. Electrochem. Soc.*, 2020, 167.
7 Y. C. Wang, S. Z. Song, J. Q. Wang, Y. Behnamian, L. K. Xu, H. Q. Fan and D. H. Xia, *J. Electrochem. Soc.*, 2019, **166**, C332–C344.

8 Z. R. Harrold, M. L. Skidmore, T. L. Hamilton, L. Desch, K. Amada, W. van Gelder, K. Glover, E. E. Roden and E. S. Boyd, *Appl. Environ. Microbiol.*, 2016, **82**, 1486–1495.
9 R. Smulik-Izydorczyk, A. Mesjasz, A. Gerbich, J. Adamus, R. Michalski and A. Sikora, *Nitric Oxide*, 2017, **69**, 61–68.
10 J. Y. Liu, X. T. Li, C. Batchelor-McAuley, G. D. Zhu and R. G. Compton, *Chem.–Eur. J.*, 2017, **23**, 17823–17828.
11 L. Zhang, S. B. Li, Z. F. Zhang, L. C. Tan, H. J. Pang and H. Y. Ma, *J. Electroanal. Chem.*, 2017, **807**, 97–103.
12 S. S. M. Hassan, S. A. Marei, I. H. Badr and H. A. Arida, *Talanta*, 2001, **54**, 773–782.
13 S. Srijaranai, R. Burakham, T. Khammeng and R. L. Deming, *Anal. Bioanal. Chem.*, 2002, **374**, 145–147.
14 Y. Miura and H. Hamada, *J. Chromatogr. A*, 1999, **850**, 153–160.
15 N. Bord, G. Cretier, J. L. Rocca, C. Bailly and J. P. Souchez, *J. Chromatogr. A*, 2005, **1100**, 223–229.
16 M. W. Stutelberg, C. V. Vinnakota, B. L. Mitchell, A. R. Monteil, S. E. Patterson and B. A. Logue, *J. Chromatogr. B: Anal. Technol. Biomed. Life Sci.*, 2014, **949**, 94–98.
17 Y. Miura, M. Hatakeyama, T. Hosino and P. R. Haddad, *J. Chromatogr. A*, 2002, **956**, 77–84.
18 Z. Keivani, M. Shabani-Nooshabadi and H. Karimi-Maleh, *J. Colloid Interface Sci.*, 2017, **507**, 11–17.
19 D. H. Deng, Y. Q. Hao, S. L. Yang, Q. Y. Han, L. Liu, Y. R. Xiang, F. B. Tu and N. Xia, *Sens. Actuators, B*, 2019, **286**, 415–420.
20 G. C. Han, X. R. Su, J. T. Hou, A. Ferranco, X. Z. Feng, R. S. Zeng, Z. C. Chen and H. B. Kraatz, *Sens. Actuators, B*, 2019, **282**, 130–136.
21 M. Shabani-Nooshabadi, M. Roostaee and F. Tahernejad-Javazmi, *J. Mol. Liq.*, 2016, **219**, 142–148.
22 J. B. Raoof, R. Ojani and H. Karimi-Maleh, *Chin. Chem. Lett.*, 2010, **21**, 1462–1466.
23 X. Z. Feng, H. F. Li, A. Ferranco, Z. C. Chen, M. Y. Xue, G. C. Han, Z. L. Jiang and H. B. Kraatz, *J. Electrochem. Soc.*, 2020, **167**, 067503.
24 X. Z. Feng, X. R. Su, A. Ferranco, Z. C. Chen, G. C. Han, Z. L. Jiang and H. B. Kraatz, *J. Biomed. Nanotechnol.*, 2020, **16**, 29–39.
25 F. Tahernejad-Javazmi and M. Shabani-Nooshabadi, *J. Electrochem. Soc.*, 2017, **164**, H975–H980.
26 V. K. Gupta, M. A. Khalilzadeh, A. Rudbaraki, S. Agarwal, M. L. Yola and N. Atar, *Int. J. Electrochem. Sci.*, 2017, **12**, 3931–3940.
27 S. Lu, M. Hummel, S. Kang and Z. R. Gu, *J. Electrochem. Soc.*, 2020, **167**, 046515.
28 L. Liu, Y. Chang, J. Yu, M. S. Jiang and N. Xia, *Sens. Actuators, B*, 2017, **251**, 359–365.
29 N. Xia, Z. H. Chen, Y. D. Liu, H. Z. Ren and L. Liu, *Sens. Actuators, B*, 2017, **243**, 784–791.
30 N. Xia, X. Wang, J. Yu, Y. Y. Wu, S. C. Cheng, Y. Xing and L. Liu, *Sens. Actuators, B*, 2017, **239**, 834–840.
31 L. L. Cao, C. Fang, R. S. Zeng, X. J. Zhao, Y. R. Jiang and Z. C. Chen, *Biosens. Bioelectron.*, 2017, **92**, 87–94.
32 L. L. Cao, C. Fang, R. S. Zeng, X. J. Zhao, F. J. Zhao, Y. R. Jiang and Z. C. Chen, *Sens. Actuators, B*, 2017, **252**, 44–54.